Master's Thesis

Uplink-Based Downlink Beamforming in Frequency Division Duplex Systems

Sahar Imtiaz

Department of Electrical and Information Technology,
Faculty of Engineering, LTH, Lund University, June 2014.

Master's Thesis

Uplink-Based Downlink Beamforming in Frequency Division Duplex Systems

By

Sahar Imtiaz

Department of Electrical and Information Technology
Faculty of Engineering, LTH, Lund University
Lund, Sweden

Abstract

Extensive research has been carried out till now on the possibility of using the channel reciprocity between the uplink and downlink channels in Frequency Division Duplex (FDD) systems to improve the systems' efficiency. Different studies have concluded differently regarding the characterization of the dissimilarity in uplink and downlink channel properties. This study focuses on analyzing the mismatch in directional properties of the uplink and downlink channels of FDD systems based on the structure of their multipath clusters. In general, the multipath components arriving at the base station are seen as clusters, rather than individual signal paths, at a system level, due to the limited directional resolution. This fact is used to describe the mismatch of directional properties between uplink and downlink. A *spectral dissimilarity metric* is introduced as a measure to characterize this mismatch and a detailed study of this dissimilarity metric is also presented. It is found that under favorable propagation conditions, for both actual channel measurement data and ray-tracing simulations, the directional and power properties of the downlink multipath clusters can be estimated from the uplink channel with high reliability. This result is further validated by calculating the sum capacity of multiuser systems using uplink based downlink channel estimation and comparing this with the sum capacity calculated by using the actual downlink channel parameters. It is found that the system sum capacity calculated using the uplink based downlink estimation differs very slightly (a maximum difference of 14%) from the actual system sum capacity, when downlink beamforming algorithm is used. Furthermore, the difference between the system sum capacities calculated using uplink channel based estimated downlink channel and the actual downlink channel properties is lesser for lesser mismatch in the cluster properties of uplink and downlink for the considered system. Therefore, directional-based beamforming transmission technique for FDD systems is able to benefit from such multipath clusters' similarity in order to improve the system performance.

Acknowledgments

This Master's thesis would not exist without the support and guidance of my examiner, Fredrik Tufvesson, who offered me the chance to conduct this thesis study in the first place. I am thankful to my thesis supervisor, Fredrik Rusek, for providing valuable comments and guidance to improve the research process in this thesis work from time to time. Also, I am extremely thankful to my thesis co-supervisor, Ghassan Dahman, whose valuable technical advice was of great help at every stage of this thesis study. His continuous guidance and appreciation kept me motivated throughout the course of my thesis.

Sahar Imtiaz

Table of Contents

CHAPTER 1

1 Introduction

This chapter gives a detailed description about the motivation of this thesis. The contributions of the findings of this work will also be elaborated. The summary of the topics to be discussed in the thesis report concludes this chapter.

1.1 Background and Motivation

Nowadays, wireless communication systems can be seen in many forms in our surroundings, their implementation in mobile handsets being the dominant one. The ever-increasing demand for better technology necessitates the efficient utilization of the available resources. In order to ensure that all users are served adequately, the transmission techniques in a wireless communication system are designed considering optimum utilization of resources in time, frequency, code, and space. Nowadays, due to widespread use of wireless communications, multiple antennas are used at the transmitter and/or the receiver to satisfy the needs of the end users. The use of multiple antennas to increase the system throughput by efficiently utilizing the spatial domain has gained much popularity in the past few years. The transmitter, known as base station (BS) in a wireless communication system, is equipped with multiple antennas that can be used to focus the transmitted signal in particular directions in spatial domain to serve the intended users. This is technically known as ‘beamforming’ and is one of the reasons for the favorable use of multiple antennas in modern wireless communication systems.

The directional information of intended users is inherently required for the implementation of beamforming. Thus it is necessary that the channel state information at the transmitter (CSIT) is readily available. In a communication system utilizing the time resource, called time division duplexing (TDD) system, CSIT is known at the transmitter; however the constraint of time-synchronization between the transmitter and the receiver has to be taken care of. In contrast, the systems utilizing the frequency resource, known as frequency division duplexing (FDD) systems, do not have the limitation of requiring tough time-synchronization for communication. In FDD, the channel realizations for communication from the transmitter to the receiver, called downlink (DL), and from the receiver to the transmitter, called uplink (UL), can be assumed to be independent of each other, because the UL and DL channels are well-separated in the frequency domain. However, the user channel state information is required to be fed back to the transmitter reliably [1]. The overhead, due to the feedback and the delay, needs to be catered for efficient system performance when multiple antennas are used.

In order to ensure that the overall system performance can be improved by using the UL directional information for DL transmission, it is necessary to characterize the mismatch in directional properties of the duplex channels. Various researchers have carried out different studies to characterize the mismatch between the directional channel properties of UL and DL in FDD systems. Different conclusions have been drawn regarding the mismatch in directional properties of duplex channels, depending on the method used for investigation of the mismatch. The authors in [2] compared only the dominant angle-of-arrival (AoA), a parameter of directional channel property, at the transmitter i.e., BS, and the receiver i.e., mobile station (MS), for both the UL and DL channels, in an outdoor environment. Their study concluded that the dominant AoAs for UL and DL channels are very similar. In [3], the first- and second-order central moments of azimuth power spectrum (APS) for UL and DL are compared and it was concluded that both are almost identical; therefore the UL channel information can be reliably used for DL channel estimation.

In [4], a super-resolution algorithm, Unitary ESPRIT [5], for 2D is used to estimate the directional properties of the multipath components (MPCs) for both the UL and DL channels. Afterwards, the complex valued APSs were compared by correlating them and it was found that no correlation exists between the APSs of UL and DL channels, since the maximum value computed for correlation was 0.20. In another study [6] based on the spatial channel measurements carried out in WCDMA of UMTS, the similarity of UL and DL directional properties was studied. The similarity of directional properties of UL and DL channels was investigated by comparing the instantaneous AoAs, as well as by correlating the APSs of duplex channels. It was concluded that the instantaneous dominant AoA, as well as the average spatial channel characteristics i.e., APS, of both UL and DL are highly correlated and thus the UL channel information can be used for beamforming in DL communication.

All of the aforementioned research findings presented the conclusions based on the study of different directional channel properties for UL and DL. Some studied only the dominant AoAs in UL and DL (as in [2]); some compared only the average spatial channel characteristics, like comparing the first- and second- order central moments of APSs of UL and DL as done in [3]; and some based their conclusions on the APSs constructed using high-resolution algorithms, like Unitary ESPRIT in [4], and Capon's beamformer in [6]. This study presents a novel way of characterizing the mismatch in UL and DL channels by using the complete set of directional properties of duplex channels, for narrowband systems. Furthermore, the overall system performance is also investigated by comparing the beamforming done on the basis of only the UL and then the DL channel information. Since this study focuses on the directional channel information, the validation of results will be carried out on the basis of directional-beamforming. From now onwards, the term beamforming will refer to the term 'directional-beamforming' throughout the document.

The multiple antennas used at the BS can be used for beamforming purpose by steering the beam of transmitted signal in the direction of intended users. Generally, two types of propagation scenarios exist between a transmitter and a receiver. One, when the transmitter is in line-of-sight (LOS) with the intended receiver, and the other when an obstruction exists between the transmitter and the receiver, resulting in non line-of-sight (NLOS) condition. In case of LOS, the location of the intended user as well its directional information is equivalent, therefore, the beam can be directly steered towards the location of the intended user using the directional information. Whereas in case of NLOS, the presence of obstructions or various interacting objects (IOs) in the surroundings results in reflecting, diffracting or scattering the transmitted signal. In this case, the signal from the transmitter reaches the intended users in the form of clusters, which are composed of groups of MPCs having same directional/delay characteristics, and remain the same during a specific space/time span.

This study focuses on avoiding the feedback in FDD systems, by utilizing the information in spatial domain from the UL for improving the DL transmission techniques. If DL beamforming transmission is used, the comparison of UL and DL channels can be done in a more meaningful way based on the multipath clusters. One reason for the benefit using this approach is that in a general propagation environment, the different MPCs arriving at the BS or MS appear to be in the form of clusters, thus it is better to characterize the mismatch in directional channel properties on the basis of multipath clusters. Also, from a system point-of-view, practically the beams can be steered in only limited directions due to limitation of beamwidth/bandwidth; therefore, the system realizes the sum of MPCs having similar directional/temporal characteristics, rather than distinguishing them individually. Hence this work presents the mismatch characterization between UL and DL channels based on the difference between instantaneous power of the multipath clusters in UL and DL channels, in order to improve the beamforming based DL transmission technique.

1.2 Contributions of this study

The prospect of the use of channel reciprocity property in FDD systems to improve the overall system performance has been a topic of interest for long. As mentioned earlier, several studies have concluded differently while trying to characterize the dissimilarity in the UL and DL channel properties. In this study, the directional properties of UL and DL channels are compared as a means to improve the beamforming based transmission technique in FDD systems. The main contributions of this study are:

- the proposal of a spectral dissimilarity metric, to characterize the dissimilarity between UL and DL directional properties based on multipath clusters, and
- the validation of the usefulness of the proposed spectral dissimilarity metric, by implementing DL beamforming transmission technique, using the information from UL multipath clusters, on the simulated data to evaluate the achievable sum-rate capacity.

1.3 Organization of thesis

This thesis is organized as follows:

- An overview of the background information related to this thesis work is described in Chapter 2;
- Chapter 3 presents the details of the methods used for extracting the data for analysis in the thesis study;
- The tools used for analyzing the data and to characterize the results are elaborated in Chapter 4;

- Chapter 5 describes the usefulness of the analysis by doing beamforming based on the information of UL multipath clusters and then comparing this with the beamforming done using the actual DL multipath channel information;
- The results of the thesis findings are presented in Chapter 6.

CHAPTER 2

2 Background Overview

This chapter describes some of the background information relevant to this thesis work. The radio channel and some of the channel characteristics are described in detail. The identification of multipath clusters is also elaborated, followed by the characterization of dissimilarity between UL and DL channels in FDD systems. The description of beamforming as one of the DL transmission techniques is presented at the end of this chapter.

2.1 The radio channel

A wireless communication system consists of three main parts; the transmitter, the receiver, and the medium in which the communication occurs. The medium is known as the “radio channel”. The transmitter is commonly known as the base station (BS) and the receiver is called the mobile station (MS). The transmitted signal from BS can reach the MS either directly, referred as LOS communication, or after interacting with different objects present between the BS and the MS, referred as NLOS communication. In NLOS communication, the transmitted signal experiences different propagation phenomena including reflection, diffraction, scattering, etc [7]. Depending on the signal interaction with various objects, the MS receives the signals arriving from various paths, thus giving rise to the term ‘multipath components’ (MPCs). Figure 1 shows two signal paths between a BS and an MS; path 1 shows LOS communication, whereas path 2 shows the signal reaching the MS after being reflected from an interacting object (IO).

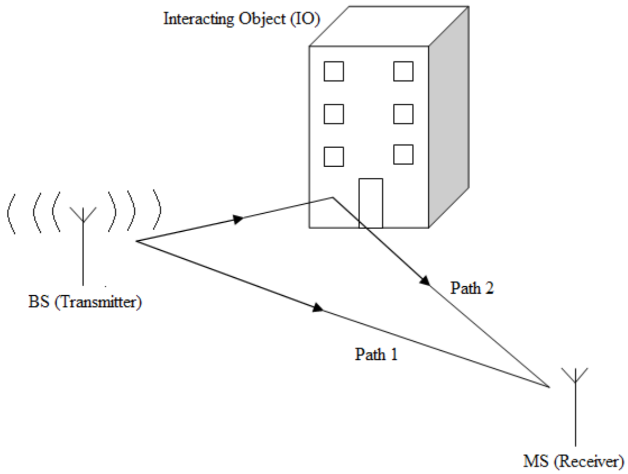

Fig. 1. Example of multipath propagation

Each MPC can be defined on the basis of a number of channel parameters. The amplitude of an MPC shows the strength of the signal when it reaches the receiver, and the phase of an MPC is related to the non-integer parts of the wavelengths it travels before reaching a receiver [8]. The directional properties of an MPC consist of the azimuth-angle-of-arrival (AAoA), elevation-angle-of-arrival (EAoA), azimuth-angle-of-departure (AAoD) and elevation-angle-of-departure (EAoD). The temporal channel properties of an MPC comprise the delay, which is the time an MPC takes to reach a receiver from a transmitter. In this work, only the amplitude, phase and the directional properties of MPCs are considered, because narrowband channel is assumed, and thus the delay is ignored for computation of the results.

2.2 The multipath clusters

In [9], the term cluster, in relation to the properties of MPCs, is explained as follows:

> "In measured MIMO propagation channels the MPCs tend to occur in clusters, i.e., groups of MPCs with similar parameters, delay, direction of arrival (DOA), and direction of departure (DOD) [10] [11]."

It has been reported in many studies related to communication systems deploying multiple antennas that the channel parameters of MPCs appear as groups, in terms of directional properties, and thus can be identified as multipath clusters [12], [13]. Generally, the visual inspection of clusters of MPCs is used to validate the grouping, however in case of large data sets, the visualization becomes cumbersome. In this work, the clustering algorithm proposed in [14] is used to group the MPCs showing similar directional properties. The algorithm presented in [14] uses the spatio-temporal characteristics of MPCs for clustering, however in this case, since narrowband system is considered, only the spatial (i.e., directional) properties are used for clustering the MPCs. The K-Power Means algorithm is applied in the same manner as done in [14] except that the **X** matrix comprises only the directional properties of the MPCs. The centroids for K clusters in the clustering algorithm are initialized randomly, and are then updated based on the distance of MPCs from the centroids. The distance of MPCs is computed in terms of their directional properties, referred to as the multipath component distance (MCD). The MCD, for the angle of arrival (AoA) or the angle of departure (AoD), of an MPC *i*, from a centroid *j*, is computed as [15]:

$$MCD_{AoA/AoD,ij} = \frac{1}{2}\left| \begin{pmatrix} \sin(\theta_i)\cos(\varphi_i) \\ \sin(\theta_i)\sin(\varphi_i) \\ \cos(\theta_i) \end{pmatrix} - \begin{pmatrix} \sin(\theta_j)\cos(\varphi_j) \\ \sin(\theta_j)\sin(\varphi_j) \\ \cos(\theta_j) \end{pmatrix} \right| , \tag{1}$$

for AoA/AoD in the same manner, but computed separately. It must be noted here that $MCD_{AoA/AoD,ij}$ is vector-valued. Here, $|...|$ denotes the absolute value of the entity; θ denotes the elevation angles and φ denotes the azimuth angles of the MPC and the centroid. The overall distance measure is given by [15]:

$$MCD_{ij} = \sqrt{\left\| MCD_{AoA,ij} \right\|^2 + \left\| MCD_{AoD,ij} \right\|^2} , \tag{2}$$

where $\|...\|$ is the length of the vector $MCD_{AoA/AoD,ij}$, and represents the distance of the two angles, elevation and azimuth angles for AoA/AoD, on the unit sphere [15]. The MPCs for both UL and DL channels are fed together as input to the K-Power Means clustering algorithm and the resulting clusters are used for further analysis.

2.3 FDD uplink and downlink channel dissimilarity

One way of increasing the overall performance of a multi-antenna system is by radiating the transmission energy in the directions exhibiting high channel gain. In FDD systems, since the UL and DL channels are well-separated in the frequency domain, therefore, the channel realizations of UL and DL are independent of each other. However, both the UL and the DL signals interact with the same environment i.e., the IOs are the same for both cases, so it can be assumed that the directional properties of DL clusters can be extracted from the dominant UL clusters. To validate this assumption, it is necessary to define a metric that can characterize the difference between the instantaneous power levels of the significant clusters of UL and DL channels.

A measure of dissimilarity, named as '*spectral dissimilarity metric*', denoted by D_{SDM}, is used to characterize the difference between the instantaneous power levels of most significant clusters in UL and DL channels. This metric is derived from the 'spectral similarity metric', defined in [16], and is given as follows:

$$D_{SDM} = \frac{\sum_{c=1}^{C} \left| S_{c,UL} - S_{c,DL} \right|}{\sum_{c=1}^{C} S_{c,UL} + \sum_{c=1}^{C} S_{c,DL}} \tag{3}$$

where,

$$S_{c,UL/DL} = \frac{\left| \sum_{l=1}^{L} \alpha_{c,l}{}^{UL/DL} \exp(j\varphi_{c,l}{}^{UL/DL}) \right|^2}{\sum_{c'=1}^{C} \left| \sum_{l=1}^{L} \alpha_{c',l}{}^{UL/DL} \exp(j\varphi_{c',l}{}^{UL/DL}) \right|^2} \, . \tag{4}$$

Here, C denotes the total number of clusters used for computing D_{SDM} and $C > 1$, $S_{c,UL}$ and $S_{c,DL}$ denote the fraction of the total instantaneous power carried by the c^{th} cluster of the UL and DL channel, respectively. L is the total number of MPCs within a cluster; $\alpha_{c,l}{}^{UL/DL}$ and $\varphi_{c,l}{}^{UL/DL}$ represent the amplitude and phase of the l^{th} MPC in the c^{th} cluster of the UL/DL, respectively. The UL and DL channel MPCs have approximately the same amplitudes, whereas the phases of the MPCs are uniformly distributed in [0, 2π] and are independent of each other. Since the total instantaneous power of the UL and the DL clusters is normalized to 1, i.e.

$$\sum_{c=1}^{C} S_{c,UL} = \sum_{c=1}^{C} S_{c,DL} = 1 \ , \tag{5}$$

therefore, (3) can be written as:

$$D_{SDM} = \frac{1}{2}\sum_{c=1}^{C} \left| S_{c,UL} - S_{c,DL} \right| \tag{6}$$

The range of this metric is from 0 to 1, i.e., when the power of the corresponding clusters in UL and DL are same, D_{SDM} will be 0, showing a perfect match, and vice versa.

The spectral similarity metric used in [16] was used to identify the changes in the characteristics of radio channel by observing the changes in the spectrum of AoA of the received signal. The AoAs of the considered channels are divided into pre-defined non-overlapping sub-intervals, and the sum of powers within each sub-interval is compared to each other using the spectral similarity metric. The function in (6) is a modified version of that similarity metric, where the comparison is made by dividing the instantaneous power among the multipath clusters, formed using directional properties, which directly relate to the structure of the propagation environment. It also has to be noted that the value of D_{SDM} depends on the number of considered clusters used for its calculation; this will be further explained in Chapter 4.

2.4 Transmission techniques

As mentioned earlier, multiple antennas are widely used nowadays to increase the throughput of the communication system. Usually, the BS is equipped with multiple antennas, and by the use of various signal processing techniques, the efficiency of the overall system can be increased manifold by serving the MSs, which can be equipped with one or more antennas, showing good channel conditions. One of the several terms used to validate the system performance is ‘capacity’, which defines the maximum rate over which the information can be transmitted over a given channel [7]. The multiple-input-multiple-output (MIMO) systems are known to achieve the best possible system capacity using spatial-multiplexing, but for its computation, it is necessary that CSIT is available [17]. One way of improving the MIMO system capacity is to utilize the spatial domain to acquire partial CSIT, i.e., the directional channel state information, and thus, improve the system throughput by transmission of signals towards specific users.

Beamforming is the technical term used to describe the transmission of signals by the BS, in spatial domain, towards specific users (or MSs) by radiating the energy in the directions of the users experiencing good channel conditions [18]. Beamforming inherently requires partial (i.e. directional) CSIT for its implementation. In this work, the information from dominant UL clusters is used to do beamforming in DL communication, and the results are compared with the beamforming done using the information from dominant DL clusters. In this way, the validity of the results obtained after analysis is further tested, and is summarized in the concluding chapters. Here, only an introduction to the beamforming technique used for validation is presented; the details of its implementation are given in Chapter 5.

This chapter presented a background overview of the work carried out during this study. The following chapter describes the methods used for collection of data, i.e., the directional properties of the MPCs and their corresponding powers, that is used for further processing.

CHAPTER 3

3 Data Collection for Analysis

This chapter describes the methods used for extracting the properties of MPCs for further analysis. Mainly, two types of methods are deployed for collection of data, namely: multi-antenna propagation measurements, and ray-tracer simulations. The details regarding the collection of MPCs and their characteristics using the aforementioned methods are given in the following sub-sections.

3.1 Propagation measurements

Two measurement campaigns were conducted to collect the data for MPCs in multi-antenna propagation scenario. Both measurements were carried out in the vicinity of the campus of Lund University, Lund, Sweden. The RUSK Lund channel sounder [19] was used for collecting the data for MPCs in both the measurement campaigns. First measurement campaign was conducted considering different propagation scenarios (namely LOS and NLOS), in which the number of scatterers was limited. The directional information of the MPCs was available at the BS, which was equipped with an antenna array, and it was placed at a height above the surrounding buildings. In the second measurement campaign, the directional information of the MPCs was available at the MS, which was equipped with an antenna array. The MS was moved along a continuous route encircling a lake and it was surrounded by many scatterers. The details for both the measurement campaigns are as follows:

3.1.1 Measurement campaign 1

The center frequency used for collecting the data in the first measurement campaign was 2.6 GHz, at a bandwidth of about 45 MHz. The measurement setup comprised of one BS, the RUSK Lund channel sounder, having 64-dual polarized antenna elements arranged in a stacked uniform cylindrical array. The BS antenna was placed at the rooftop of a four-storey building, at the location indicated in Figure 2. The MS consisted of a single omni-directional antenna and was placed at a height of 1.84 m from the ground.

The transmitted power was 27 dBm. More details about the measurement setup can be found in [20].

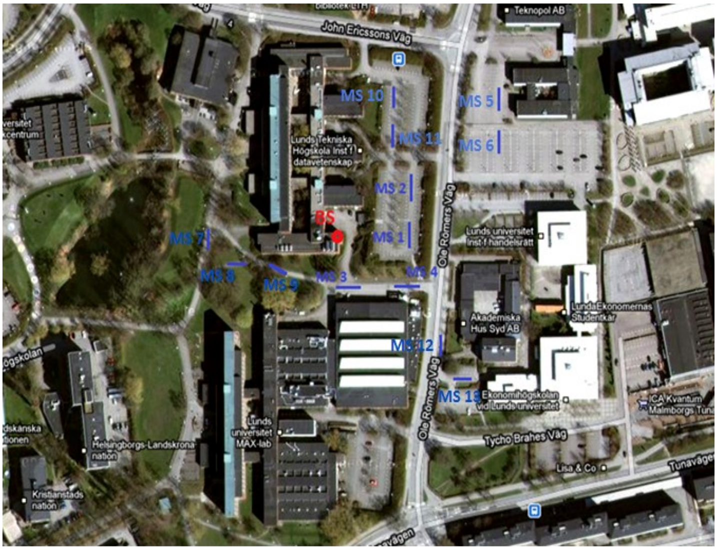

Fig. 2. Aerial view of the measurement area; red circle shows the location of BS, MS locations are indicated by labels in blue color

Every measurement location of MS indicated in Figure 2 is a pre-defined path of distance 20 m, along which the MS was dragged with a speed of about 0.5 m/s. Each of the MS locations denotes 5 parallel paths along which the MS was dragged, where each path is separated by 0.5 m, and for each path 40 snapshots were measured. As shown in Figure 2, 13 MS locations were used, each having 5 parallel paths. Therefore, 2600 snapshots were collected altogether and are used for further processing. As mentioned earlier, the propagation scenarios were considered for both LOS and NLOS communication. It should be noted that the stacked uniform cylindrical array acting as BS, used for collecting the MPCs data, is located in an isolated position with respect to the surrounding scatterers. Therefore, the MPC parameters are expected to have lesser dispersion.

The raw measurement data recorded at the channel sounder consists of transfer functions between each transmission link, thus it can be considered as multiple-input single-output (MISO) channel, for each MS location. 141 frequency points within a bandwidth of 43.75 MHz make a single MISO transfer function. From the collected data, each 20th frequency bin, with inter-bin spacing of 6.25 MHz, is used for further processing. The DL channel is represented by the first frequency bin, and all of the other frequency bins are subsequently considered as UL channels, corresponding to duplex distances of 6.25 MHz to 43.75 MHz, with 6.25 MHz as step distance. Each of the collected 2600 snapshots has 9 MISO transfer functions, having a dimensionality of 128 BS antennas × 1 MS antenna each. Finally, each MISO transfer function is processed using SAGE algorithm to extract the required parameters for each MPC. The extracted MPC parameters are azimuth-angle-of-departure (AAoD), elevation-angle-of-departure (EAoD), and complex amplitude.

3.1.2 Measurement campaign 2

Another measurement campaign was conducted in a different propagation environment, having many scatterers, but in the same surroundings. The center frequency was set to be 2.6 GHz and the measurement bandwidth was 40 MHz. The measurement setup comprised of remotely located four BSs used as transmitters, each equipped with a single vertically polarized antenna element. All four transmitting BSs were interlinked via the optical backbone network of the campus, through which the sounding signal was conveyed using the radio-over-fiber (RoF) transceivers. The transmission signal was broadcasted by the BSs, which was received by a single MS having 64 dual-polarized antenna elements in a stacked uniform cylindrical array configuration. It should be noted that the directional properties of the MPCs are available at the MS which is lower than the surrounding IOs, mainly trees. In total, 512 (4 BSs × 128 MS antenna elements) transmit-receive channels were sounded using time-multiplexing, where all receive antenna elements were visited in succession before switching to the next transmit antenna element. This process resulted in the collection of one *snapshot* of the data. The channel sounder was wheel-triggered at one snapshot per wavelength. Further details regarding the measurement setup and the equipment used can be found in [21].

The placement of transmit antennas was such that each antenna was facing out from the windows of the rooms located at the second or third floors of four different buildings. The measurements were recorded using the channel sounder in an open area encircling a small lake, and surrounded by the selected four buildings and tall leafy trees, as shown in Figure 3. In this case, since the MS is surrounded by many scatterers, the MPC parameters are expected to have more spread of the values. The total length of measurement route was 490 m, which corresponds to 4200 snapshots; however, in this work only each tenth snapshot is considered for further analysis. The propagation conditions between the MS and each of the BSs can be characterized as obstructed line-of-sight (OLOS) or NLOS due to the presence of large leafy trees in the measurement area.

The raw data obtained from the measurements at the channel sounder consist of the transfer functions between each transmit-receive link, i.e., it can be characterized as single-input-multiple-output (SIMO) channel, for each of the four links. Each measured SIMO transfer function consists of 513 frequency points covering the 40 MHz measurement bandwidth. In this work, each 64^{th} frequency bin, with inter-bin distance of 5 MHz, is selected for further analysis; in all, 9 frequency bins are considered. The first frequency bin is chosen to represent the DL channel, and each one of the rest of the frequency bins are sequentially selected to represent the UL channel, which is corresponding to duplex distances of 5 MHz to 40 MHz in steps of 5 MHz. The total number of obtained snapshots is therefore 4×420 = 1680, where each snapshot comprises 9 SIMO transfer functions (corresponding to the 9 frequency bins), and each SIMO transfer function has the dimensionality of 128 receiver (Rx) antennas × 1 transmitter (Tx) antenna. Then, the SAGE algorithm was applied to each SIMO transfer function in order to extract the azimuth-angle-of-arrival (AAoA), elevation-angle-of-arrival (EAoA), and complex amplitude of each MPC.

Fig. 3. Aerial view of the measurement area for measurement campaign 2; BS locations are indicated by labels BS-E, BS-S, BS-F and BS-M. The measurement route is highlighted in blue color

3.2 Ray-tracing simulations

The ray-tracing simulations are carried out using the commercial ray-tracer, 'Wireless InSite', developed by Remcom. In order to simulate a typical urban propagation environment, the 3D model of downtown of Helsinki city, Finland, is used. In an open area located near the middle of the 3D model, a BS was placed at a height of 20 m from the ground. A set of 228 MSs were placed in the form of a route to simulate the propagation paths for different locations of an MS. Each MS has a height of 1.5 m from the ground and is separated by a distance of 5 m from each other. The 3D model used for simulations, along with the placement of BS and MSs is shown in Figure 4.

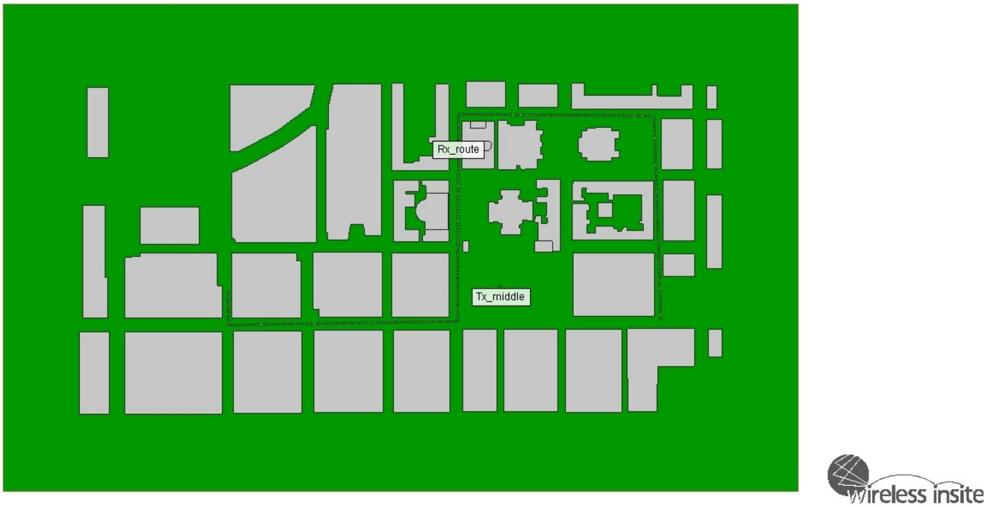

Fig. 4. 3D model of downtown Helsinki, Finland, used for ray-tracer simulations

For simulations, the frequency band for E-UTRA band 7 [22] is used, having center frequency of 2.6 GHz. The duplex distances used for simulations vary from 5 MHz to 120 MHz. Both the BS and MS antennas are chosen to be isotropic. The 'full 3D' propagation model is used for simulations, in which the height of the BS and MS is independent of any other simulation/model parameters. The maximum number of reflections was set to be 10, and the total number of diffractions allowed for any simulated propagation path is 2. No wave transmission through the buildings is considered. The Shooting and Bouncing Ray (SBR) was used as ray-tracing method for the selected propagation model [23], in which the ray paths are traced through the two-dimensional building geometry regardless of the location of specific field points. The ray-tracing tool simulates specular rays for any propagation path and each specularly reflected ray from the building walls is traced up to either the maximum number of reflections specified for simulation, or when it hits the boundary of the study area of ray-tracing simulation model. The parameters extracted for each MPC from the simulation output files are AAoD, EAoD, AAoA and EAoA, and the complex amplitude.

Table 1 summarizes the different parameter settings used for all the methods from which the information about MPCs is extracted.

TABLE 1. PARAMETER SETTINGS FOR PROPAGATION MEASUREMENTS AND RAY-TRACER SIMULATIONS

Parameter	Measurement Campaign 1	Measurement Campaign 2	Ray Tracing
Propagation Envirnoment	Suburban	Suburban	Urban
Duplex Distances	6.25 to 43.75 MHz in steps of 6.25 MHz	5 to 40 MHz in steps of 5 MHz	5, 10, 20, 40, 60, 80, 100, 120 MHz
Parameters used to describe MPCs	Complex amplitude, AAoD[1], EAoD[1]	Complex amplitude, AAoA[1], EAoA[1]	Complex amplitude, AAoA[1], EAoA[1], AAoD[1], EAoD[1]
Antenna Polarization	Vertical	Vertical	Vertical

1. Azimuth-Angle-of-Arrival (AAoA), Elevation-Angle-of-Arrival (EAoA), Azimuth-Angle-of-Departure (AAoD), Elevation-Angle-of-Departure (EAoD)

This chapter presented the details about the methods used for extracting the MPC parameters, i.e., multi-antenna propagation measurements and ray-tracer simulations. The next chapter describes the tools used for further processing, characterizing and analyzing the data.

CHAPTER 4

4 Characterizing the Uplink and Downlink Channel Dissimilarity

The previous chapter presented the details about the methods used for collecting the parameters of MPCs, for further processing and analysis. This chapter provides a detailed description of the processing and analysis tools, used for extracting some results of this study. The MPC parameters are first classified in the form of clusters, using the clustering algorithm described in the following sub-section. Afterwards, the clustered MPCs are analyzed using a dissimilarity metric, which is explained at the end of this chapter.

4.1 Processing the data using K-power means clustering

The MPC parameters obtained from both the multi-antenna propagation measurements and the ray-tracing simulations are further processed using a clustering algorithm. In this study, the K-power means clustering algorithm is used to classify the MPCs into multipath clusters [14]. The power properties and the spatial characteristics of MPCs are used as input to the clustering algorithm. As mentioned earlier, since a narrowband system is considered, therefore the delay associated with the MPCs is not used in this study.

The spatial (angular) characteristics of multipath clusters depend on the location and nature of the physical IOs present in the propagation environment. These angular characteristics do not change significantly if the separation between the duplex channels is of the order of tens of MHz. For the UL and DL channels separated by tens of MHz of frequency, the multipath clusters (almost) always posses the same directional properties, i.e. AoA and AoD; however, the power of the clusters will be different due to the different phases of the MPCs, within the cluster, at different frequencies. Therefore, the clustering is done for the UL and DL MPCs considered altogether. In this way, a multipath cluster is identified as the collection of all MPCs associated with the same IO. The parameters of

MPCs used for clustering, for the measurement data as well as the ray-tracing simulations, are elaborated in the following sub-sections.

4.1.1 Measurement data

As mentioned in the previous chapter, two measurement campaigns were carried out to collect the data for MPCs for multi-antenna propagation. Since the measurements are recorded only at the cylindrical array, which was used as the BS in first set of measurements and as MS in the second measurement campaign, the partial set of directional properties are available for further processing. From the first measurement campaign, the AAoD, EAoD and complex amplitudes are used as input to the clustering algorithm; whereas from the second measurement campaign, AAoA, EAoA and complex amplitudes are being input to the clustering algorithm.

Figure 5 shows a sample of the results of the clustering algorithm obtained for both the measurement campaigns. In the figure, the power levels of the MPCs within a cluster are represented by the size of the circles; the greater the circle's size, the greater the power level of the MPC and vice versa. It can be observed from Figure 5 that the number of MPCs within the clusters is greater for the measurement campaign 2, than those for measurement campaign 1. This is due to the difference of the location of the cylindrical array with respect to the location of IOs in the surroundings, for the two measurements. In the measurement campaign 1, the BS, equipped with the cylindrical array, is placed at a location where it is almost isolated from the scatterers, like short trees or bushes, in the surroundings. In case of the second measurement campaign, the MS, equipped with the cylindrical array, was surrounded by tall leafy trees and a large number of interacting objects, which led to the possibility of MPCs arriving from almost all direction in the azimuth plane, and thus led to larger dispersion of values of the MPCs' parameters. Also, for the latter case, the number of diffused MPCs is larger as compared to the specular components due to interaction with different IOs in the surrounding environment. Therefore, many weaker MPCs can be seen in Figure 5 (b) as compared to those in Figure 5 (a).

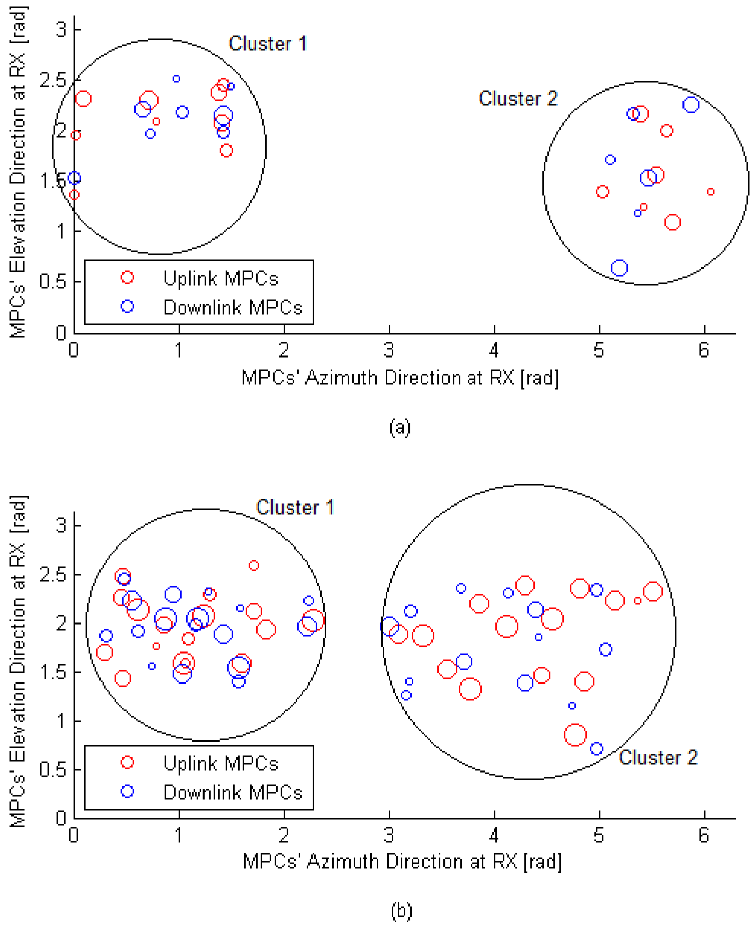

Fig. 5. Clustering of MPCs using directional properties for a snapshot of measurement data from (a) measurement campaign 1, and (b) measurement campaign 2

4.1.2 Ray-tracing data

The ray-tracing simulations generated the output files having the data for AAoA, EAoA, AAoD, EAoD and complex amplitudes of all MPCs, for both UL and DL channels. All these MPC parameters are used as input to the K-power means clustering algorithm, and the resulting clusters are used for further analysis. Figure 6 shows the clusters for one receiver location, for one duplex distance. The sizes of the circles show the power levels of the MPCs within a cluster, in the same way as in Figure 5. It can be seen from Figure 6 that the number of MPCs within a cluster is far lesser than those obtained for measurement data sets. This is because in the ray-tracing simulations, only the specular components are considered.

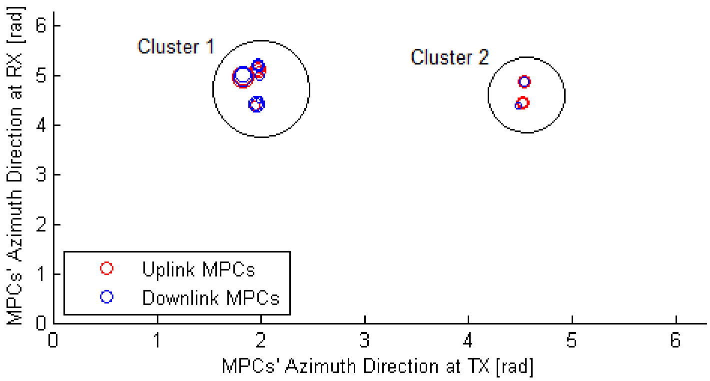

Fig. 6. Clustering of MPCs using directional properties for a receiver location in ray-tracer simulation

4.2 Analysis using the spectral dissimilarity metric

After processing the data for MPC parameters through the clustering algorithm, the mismatch in the instantaneous power carried by the UL and DL clusters is evaluated using the spectral dissimilarity metric, as mentioned in chapter 2 previously, given by:

$$D_{SDM} = \frac{1}{2}\sum_{c=1}^{C}\left|S_{c,UL} - S_{c,DL}\right| \tag{6}$$

where,

$$S_{c,UL/DL} = \frac{\left|\sum_{l=1}^{L}\alpha_{c,l}{}^{UL/DL}\exp(j\varphi_{c,l}{}^{UL/DL})\right|^2}{\sum_{c'=1}^{C}\left|\sum_{l=1}^{L}\alpha_{c',l}{}^{UL/DL}\exp(j\varphi_{c',l}{}^{UL/DL})\right|^2}\ . \tag{4}$$

As can be seen from (6), D_{SDM} depends on the number of clusters considered during its computation. Since on a system level, the strongest UL clusters are effectively considered for DL channel estimation, therefore, only the significant clusters are used for computing D_{SDM}. In order to see the effect of the number of clusters on the dissimilarity metric, the cumulative distribution function (CDF) of D_{SDM} is plotted for the clusters obtained from the measurements and simulation data. The analysis of the results is detailed in the sections below.

4.2.1 Measurement data

Figure 7 and 8 show the CDF plots of D_{SDM}, computed using the clusters obtained for both sets of measured data. The maximum number of clusters obtained for the first set of measurement data is 23, whereas for the second measurement data set, it is 15. The CDF of D_{SDM} is plotted to see the effect of using 2, 3 and 4 strongest clusters for computing D_{SDM}. It can be seen from Figures 7 and 8 that the value of D_{SDM} increases as more number of clusters is considered for computing D_{SDM}; however the increase in the value of D_{SDM} is insignificant. In terms of different duplex distances, the mismatch between the instantaneous power of UL and DL clusters does not change significantly with increasing duplex distances. The different frequencies of communication links result in different phases for the MPCs in a propagation environment, and the summation of power of MPCs defines the power of a cluster. All of the considered duplex distances, ranging from 5 MHz to 43.75 MHz, are large enough such that the effect of different frequencies is translated into statistically identical phases of MPCs.

It can also be noted that the values of D_{SDM} for both measurement data sets are quite different. This is because of the difference in the propagation environment where the measurements are done. In the first measurement campaign, the channel sounder is placed at a location where it is almost isolated from the surrounding scatterers, including short trees, bushes or a few buildings; this led to the fact that MPC parameters are having lesser spread in terms of spatial properties. Whereas in the second campaign, the channel sounder was closer to the vicinity of the scatterers, which included the tall leafy trees, the buildings as well as the vegetation surrounding the lake. The closer the scatterers are to the channel sounder, the more is the chance of the spatial properties of MPCs to be dispersive and thus, having a larger spread. Since the presence of many IOs and scatterers in the area where channel measurements are done leads to greater possibility of different wave interactions (like reflection, diffraction, scattering, etc.); therefore, the data sets from the second measurement campaign had more diffuse MPCs as compared to the ones obtained from the first measurement campaign. Consequently, the dissimilarity in the instantaneous power level of the UL and DL clusters is more for the second data set, as compared to the first one.

In general, the plots in Figures 7 and 8 show the same trend. The data from the first measurement campaign shows that for all duplex distances, the

D_{SDM} is less than 0.17, 50% of the time, considering 2 clusters only. However, when 3 and 4 clusters are considered, this value increases to 0.23 and 0.25, respectively. For the multipath clusters extracted from the second measurement campaign's data set, the D_{SDM} is less than 0.32 for 50% of the time, for all duplex distances. This increase to 0.44 and 0.5, for 3 and 4 clusters used for computing D_{SDM}, respectively, thus showing poorer results than those obtained for 2 clusters.

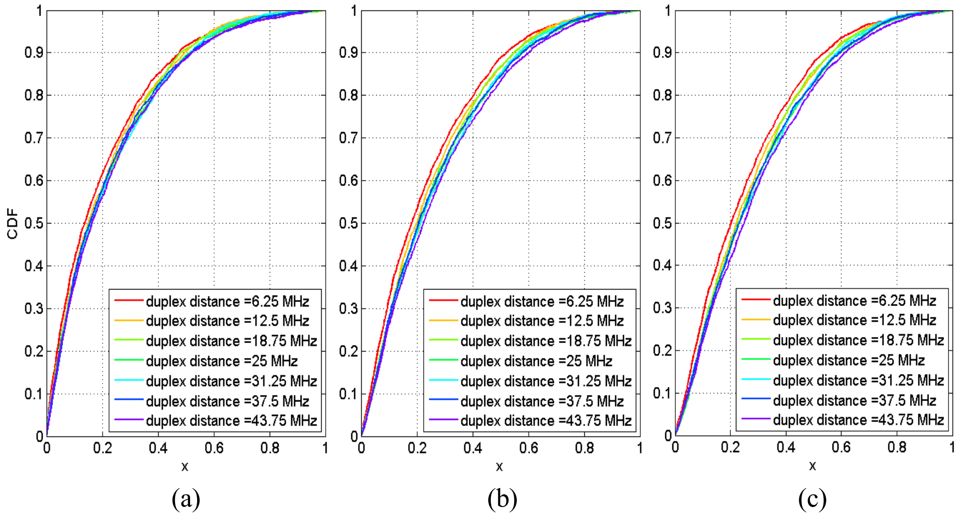

Fig. 7. Plot of CDF of spectral dissimilarity metric for (a) 2 clusters, (b) 3 clusters, (c) 4 clusters, for measurement dataset 1, for all duplex distances

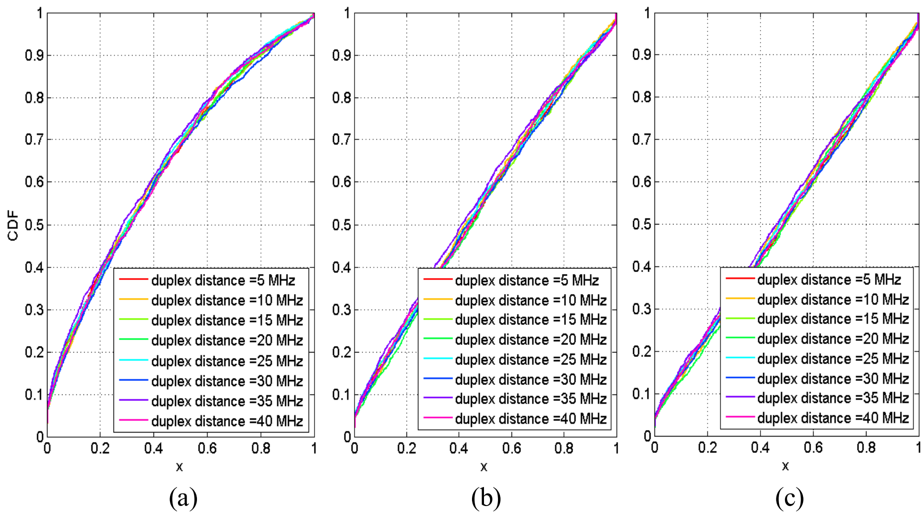

Fig. 8. Plot of CDF of spectral dissimilarity metric for (a) 2 clusters, (b) 3 clusters, (c) 4 clusters, for measurement dataset 2, for all duplex distances

4.2.2 Ray-tracing data

The data from the ray-tracing simulations is analyzed in the same way as done for the measurement data sets. The clusters obtained after processing the MPC parameters using the K-power means clustering algorithm are analyzed using the spectral dissimilarity metric. The significant 2, 3 and 4 clusters are used for computing the D_{SDM} for all receiver locations, for all duplex distances. Figure 9 shows the CDF of D_{SDM} obtained using 2, 3 and 4 clusters for its computation. In general, the same observations are made here as were for the results from the actual measurement data. The only difference is in the value of D_{SDM} obtained for its CDF for 2, 3 and 4 clusters. Since in the simulations, only the specular components are considered for ray-tracing, therefore lesser difference in terms of instantaneous power levels of UL and DL clusters is expected. From Figure 9, for 50% of the time, for all receiver locations, for all duplex distances, the D_{SDM} is less than 0.08 when only the 2 significant clusters are used for its computation. When 3 and 4 clusters are used for computing D_{SDM}, the dissimilarity increases to 0.13 and 0.14, respectively; thus again showing poor results than those obtained with 2 clusters.

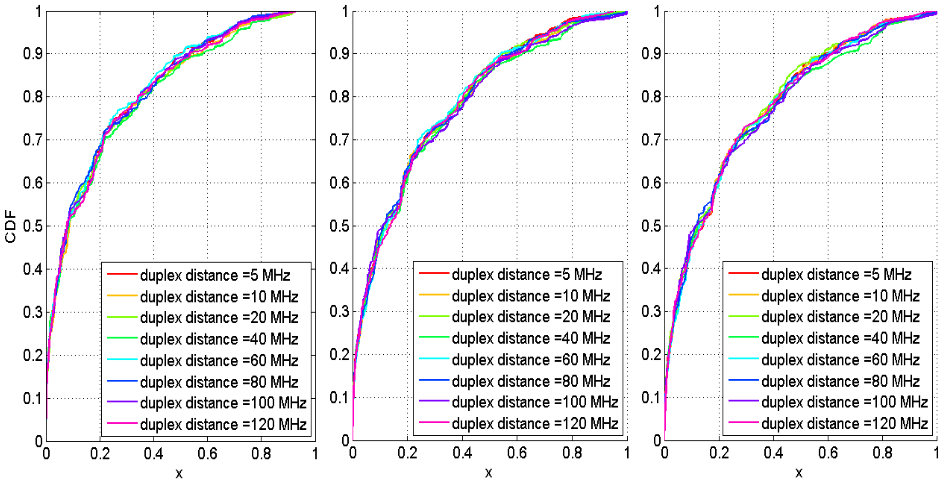

(a) (b) (c)

Fig. 9. Plot of CDF of spectral dissimilarity metric for (a) 2 clusters, (b) 3 clusters, (c) 4 clusters, for simulated data for all receiver locations, for all duplex distances

4.3 Discussion on the spectral dissimilarity metric

Table 2 shows the values of spectral dissimilarity metric, D_{SDM}, for different number of clusters, for all the methods used for collecting the

MPC data. As observed from the aforementioned results, the spectral dissimilarity metric depends on a number of factors. From Table 2, it can be seen that the value of D_{SDM} increases as the number of clusters used for its computation increases; however, this increase is not very significant. The difference in propagation environment where data is collected is a prime factor affecting the D_{SDM}. Greater the presence of diffuse MPCs in the data, greater will be the dissimilarity in power of UL and DL clusters, and thus greater will be the value of D_{SDM}. In general, the spectral dissimilarity metric is a handy tool for charactering the mismatch in UL and DL cluster characteristics. The results from the measurement data and the ray-tracing simulations show that the directional and power properties of UL clusters can be effectively used for DL beamforming, and thus the power in the DL can be radiated in the favorable direction with high reliability using the UL channel estimation.

TABLE 2. CDF VALUES FOR SPECTRAL DISSIMILARITY METRIC FOR MEASUREMEMTS AND SIMULATION DATA

CDF percentile	**Values of Spectral Dissimilarity Metric for all Duplex Distances for Different Number of Clusters (cls)**								
	Measurement Campaign 1			**Measurement Campaign 2**			**Ray Tracing**		
	2 cls	**3 cls**	**4 cls**	**2 cls**	**3 cls**	**4 cls**	**2 cls**	**3 cls**	**4 cls**
0.5	0.16	0.22	0.25	0.32	0.45	0.50	0.08	0.13	0.15
0.6	0.22	0.28	0.31	0.41	0.55	0.61	0.17	0.20	0.20
0.7	0.30	0.36	0.39	0.52	0.66	0.72	0.22	0.29	0.30
0.8	0.39	0.46	0.48	0.65	0.78	0.83	0.38	0.43	0.44
0.9	0.52	0.60	0.61	0.82	0.90	0.93	0.58	0.62	0.66

Besides this, the spectral dissimilarity metric can be used to characterize the instantaneous cluster power contribution based on the MPCs' parameters. When a cluster has only a single dominant MPC, it can be seen from (4) that the phase of that dominant MPC is not significant in computing that cluster's power. In such a case, the D_{SDM} will be effectively 0. In the other case, when a cluster has several dominant MPCs, the phase of each MPC will be significant in determining that cluster's instantaneous power. In case of LOS propagation scenario, with the amplitudes of MPCs having high K-factor, the phases of such MPCs will not be of importance while computing the cluster's power using (4). However it should be noted that having the information about the K-factors does not help in having favorable conclusive remarks about the characterization of mismatch between UL and DL clusters using D_{SDM}.

This chapter covered the details of the tools used for processing and analyzing the MPC parameters, obtained from both the actual channel measurements and the ray-tracing simulations. The results show that the directional and instantaneous power properties of the UL clusters can be favorably used for DL channel estimation under favorable propagation scenarios. This will be validated using the implementation of beamforming technique on a simulation data set, as detailed in the next chapter.

CHAPTER 5

5 Downlink Transmission Based on Uplink Directional Properties in FDD Systems

The previous chapters introduced the spectral dissimilarity metric, which classifies the mismatch in directional properties of UL and DL in FDD systems, based on the properties of multipath clusters. This chapter presents the validation of the usefulness of the introduced metric, by implementing a direction-based beamforming transmission technique utilizing the similarity between the multipath clusters of the UL and DL channels. The evaluation of performance of the proposed beamforming algorithm is done using ray-tracing data. This chapter provides the details regarding the implementation of the proposed beamforming technique and its performance evaluation. The parameter settings used for generating the simulation data are elaborated, followed by the details regarding the implementation of the beamforming using directional information. The chapter concludes with the discussion on the achieved sum-rate capacity and its relationship with the spectral dissimilarity metric.

5.1 Simulation data set for implementing the beamforming algorithm

The simulation data is generated using the parameter settings as outlined in Table 3. The same 3D model of downtown Helsinki, Finland, is used as done earlier for the ray-tracer simulations for extracting the MPC parameters (the details are mentioned in Chapter 3, section 3.2). The BS is placed at an open area located close to the center of the 3D model, with a height of 20 m from the ground, and is shown by a red colored dot in Figure 10. The black little dots in Figure 10 represent the simulated Rx positions, which spread out across the entire model. In the street canyons, the receivers are placed in the form of routes with 1 m separation. In the open area located at the top left corner of the model, the receivers are spread out in random positions. The height of each receiver is 1.5 m from the ground.

In this simulation, each Rx position represents the location of an assumed user. A total of 3,643 Rx locations, representing all the possible users' positions within the considered area, are simulated. For each Rx position, the associated MPC parameters for the UL and DL channels are extracted from the generated ray-tracer output files. Figure 10 shows the simulation model used for generating the UL and the DL channel information for different Rx positions. All other parameter settings, including the propagation model, ray-tracing method, etc., are the same as given in Chapter 3, section 3.2.

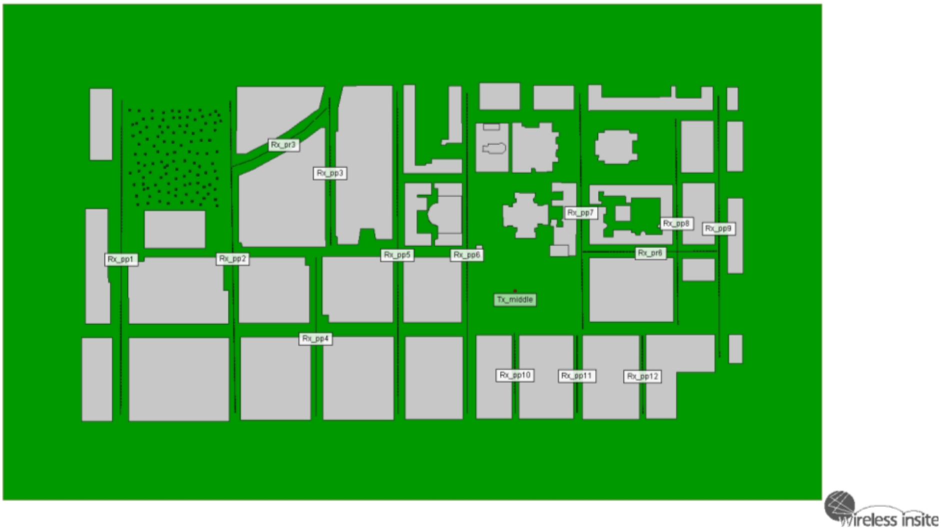

Fig. 10. 3D model of downtown Helsinki, Finland, used for generating data for beamforming; location of the BS is denoted by red color; black little dots represent the simulated Rx positions (i.e., possible users' positions)

TABLE 3. PARAMETER SETTINGS FOR SIMULATION DATA USED FOR BEAMFORMING

Parameter	Ray Tracing
Propagation Envirnoment	Urban
UL frequency	2.5 GHz
DL frequency	2.62 GHz
Parameters used to describe MPCs	Complex amplitude, AAoA[1], AAoD[1]
Antenna Polarization	Vertical

1. Azimuth-Angle-of-Arrival (AAoA), Azimuth-Angle-of-Departure (AAoD)

5.2 Downlink beamforming based on uplink directional information

In this section, we are interested in developing a directional beamforming transmission technique for multi-user communication that has the following properties:

- First, it can operate efficiently in FDD systems without the need for feedback channel information. This is done by utilizing the UL channel in order to determine the parameters that are required for the DL transmission.
- Second, it is directional based such that its goal is to transmit the DL signal in the "best directions" that maximize the sum-rate capacity of the served users.

As it has been described earlier, the UL or DL channel is described as a group of multipath clusters, each of which has its direction and power. Therefore, the success of our proposed beamformer will heavily depend on the probability of determining the direction of the strongest DL multipath clusters of the served users based on their UL multipath clusters (i.e., UL channel information).

5.2.1 The beamforming algorithm

Let us assume a system having a BS equipped with multiple antennas. In our implementation, without loss of generality, we assume having an N-element uniform circular array (UCA) at the BS. We have U available users; each is equipped with a single antenna element. Let V be the set of users selected to be served by the BS at a particular time, where size of $V = min\ (N, U)$. Hence, the channel coefficient vector of each user in V for DL, denoted by $\mathbf{h}_{v,DL}$, can be related to the AoD at the BS of the various MPCs, in case of a UCA, as [24, 25]:

$$\mathbf{h}_{v,DL} = \sum_{l=1}^{L} \alpha_l^{DL} e^{j\varphi_l^{DL}} \mathbf{SV}_{\lambda_{DL}}(\phi_l^{DL}), \tag{7}$$

where,

$$\mathbf{SV}_{\lambda_{DL}}(\phi_l^{DL}) = [e^{jk_{DL} a \sin\vartheta_l^{DL} \cos(\phi_l^{DL} - \phi_1)}, \dots\dots\dots, e^{jk_{DL} a \sin\vartheta_l^{DL} \cos(\phi_l^{DL} - \phi_N)}]^T. \tag{8}$$

Here, $\mathbf{SV}_{\lambda_{DL}}(\phi_l^{DL})$ is the steering vector associated with the DL channel having the wavelength λ_{DL}, ϕ_n denotes the angular position of the n^{th} array element of UCA, and is given as:

$$\phi_n = 2\pi n / N, \qquad n = 1,2,\dots,N \tag{9}$$

a is the radius of the array, k_{DL} is the wavenumber associated with the corresponding wavelength λ_{DL}, and $k_{DL} = 2\pi / \lambda_{DL}$. L is the total number of MPCs; $\alpha_l^{DL}, \varphi_l^{DL}, \vartheta_l^{DL}$ and ϕ_l^{DL} denote the complex amplitude, phase, elevation angle at the BS, i.e. EAoD, and azimuth angle at the BS, i.e. AAoD, of the l^{th} MPC for the DL, respectively. $[\dots]^T$ denotes the transpose of the vector.

Similarly, the channel coefficient vector for each user in V for UL communication, $\mathbf{h}_{v,UL}$, at the BS, can be related to the AoA as follows:

$$\mathbf{h}_{v,UL} = \sum_{l=1}^{L} \alpha_l^{UL} e^{j\varphi_l^{UL}} \mathbf{SV}_{\lambda_{UL}}(\phi_l^{UL}), \tag{10}$$

where,

$$\mathbf{SV}_{\lambda_{UL}}(\phi_l^{UL}) = [e^{jk_{UL}a\sin\vartheta_l^{UL}\cos(\phi_l^{UL}-\phi_1)},........., e^{jk_{UL}a\sin\vartheta_l^{UL}\cos(\phi_l^{UL}-\phi_N)}]^T. \quad (11)$$

Here, $\alpha_l^{UL}, \varphi_l^{UL}, \vartheta_l^{UL}$ and ϕ_l^{UL} denote the complex amplitude, phase, elevation angle at the BS, i.e. EAoA, and azimuth angle at the BS, i.e. AAoA, of the l^{th} MPC for the UL, respectively. k_{UL} is the wavenumber associated with the corresponding wavelength λ_{UL}, and $k_{UL} = 2\pi / \lambda_{UL}$.

Propagation measurement results have reported that the received signal energy is concentrated around the azimuth plane [26]. Furthermore, the UCA has weaker resolution in the elevation plane. Therefore, when performing beamforming, the steering vectors used at the UCA at BS have the elevation angles set to *π/2*, i.e. $\vartheta = \pi / 2$. So, the steering vectors used for beamforming, for DL or UL, at the BS are as follows [24]:

$$\mathbf{SV}_{\lambda_{DL/UL}}(\phi) = [e^{jk_{DL/UL}a\cos(\phi-\phi_1)},........., e^{jk_{DL/UL}a\cos(\phi-\phi_N)}]^T. \quad (12)$$

The information for the direction of the strongest beam serving the v^{th} user, Φ_v, for DL or UL, is embedded in the channel coefficients [18], $\mathbf{h}_{v,DL}$ or $\mathbf{h}_{v,UL}$, and that direction can be extracted using a simple beamscan [25]:

$$\Phi_{v,DL} = \arg \max_{0\le\phi<2\pi} \left| \left(\mathbf{SV}_{\lambda_{DL}}(\phi)\right)^H \mathbf{h}_{v,DL} \right| , \quad (13.a)$$

$$\Phi_{v,UL} = \arg \max_{0\le\phi<2\pi} \left| \left(\mathbf{SV}_{\lambda_{UL}}(\phi)\right)^H \mathbf{h}_{v,UL} \right| . \quad (13.b)$$

Here, $(\ldots)^H$ denotes the Hermitian transpose. It should be noted here that $\mathbf{h}_{v,DL/UL}$ denotes the summation of power of all the MPCs in the DL/UL; in other words it shows the summation of power of all multipath clusters in the DL/UL. The direction of the strongest beam for the v^{th} user, Φ_v, depends on the direction of the strongest cluster in the DL/UL, which will have the greatest influence on the value of $\mathbf{h}_{v,DL/UL}$; thus, in this way the information for all clusters is embedded in $\mathbf{h}_{v,DL/UL}$, from which the direction of the strongest cluster is being extracted using (13.a) and (13.b) for further processing.

The steering vector of the UCA determines the direction in which the BS focuses a beam towards the intended user. It should be noted that estimating the direction at the BS in which a specific user gets the strongest possible signal is done in two different ways:

- **Case 1:** This is the reference case to which we will compare the performance of our proposed algorithm. In this case, we assume that the full channel state information (CSI) is available at the BS. In other words, we assume that the BS has full information about the DL channel. Therefore, in this reference case, estimating the best direction to serve a specific user (or a group of users simultaneously) will be performed based on the DL channel, as in (13.a).
- **Case 2:** In this case, we assume that only the UL channel information is available at the BS. Therefore, estimating the best direction to serve a specific user (or a group of users simultaneously) will be performed based on the UL channel using (13.b). This case represents the estimation procedure which is performed in our proposed algorithm.

We are interested in comparing the sum-rate capacity achieved by the two above mentioned cases.

5.2.2 Computation of sum-rate capacity

We consider a multi-user case, where we assume U available users. Given that we have N BS antennas, we can serve a maximum of N users simultaneously. If $U \leq N$, then the set of users selected to be served by the BS will be $V = U$. If $U > N$, then the set of users selected to be served by the BS, V, is selected in such a way that the selected set of users will maximize the sum rate capacity. The achievable sum-rate capacity for case 1 and case 2 is calculated using the following procedure:

- **Evaluation step**: First, the signal-to-noise-and-interference ratio (SINR) for DL (case 1) and UL (case 2), $SINR_{v,DL/UL}$, for a set of randomly selected users from the U available users, V, is calculated using the channel coefficient vectors for DL and UL, for each user v, using the following equation:

$$SINR_{v,DL/UL} = \frac{\left|\left(\mathbf{S}\,\mathbf{V}_{v,\lambda_{DL/UL}}(\Phi_{v,DL/UL})\right)^H \mathbf{h}_{v,DL/UL}\right|^2}{1/\rho + \sum_{\substack{w=1 \\ w\neq v}}^{V} \left|\left(\mathbf{S}\,\mathbf{V}_{w,\lambda_{DL/UL}}(\Phi_{w,DL/UL})\right)^H \mathbf{h}_{v,DL/UL}\right|^2} \;. \tag{14}$$

The sum capacity is then calculated by:

$$R_{DL/UL} = \sum_{v=1}^{V} \log_2(1 + SINR_{v,DL/UL}) \;. \tag{15}$$

For $U > N$, this procedure is repeated a random number of times, e.g. 20 times, and the values for sum rate capacity for each selected set is saved for further processing.

- **Decision step**: For case 1, for $U \leq N$, the sum capacity will be

$$R_{case1} = R_{DL} \;. \tag{16}$$

For case 1, for $U > N$, the maximum of the sum capacity obtained at the evaluation step for 20 random trials is used to select the set of users to be served when full CSI is available at the BS, i.e.,

$$R_{case1} = \max(R_{DL,trials}) \;. \tag{17}$$

For case 2, the set of users for which the maximum sum capacity in UL is obtained is used for further processing for $U > N$. For $U \leq N$, the same set of users V is used for further processing as used at the evaluation step. The SINR for case 2 is calculated using the following equation:

$$SINR_{v} = \frac{\left|\left(\mathbf{S}\,\mathbf{V}_{v,\lambda_{DL}}(\Phi_{v,UL})\right)^H \mathbf{h}_{v,DL}\right|^2}{1/\rho + \sum_{\substack{w=1 \\ w\neq v}}^{V} \left|\left(\mathbf{S}\,\mathbf{V}_{w,\lambda_{DL}}(\Phi_{w,UL})\right)^H \mathbf{h}_{v,DL}\right|^2} \;. \tag{18}$$

The sum capacity for case 2 is then calculated by:

$$R_{case2} = \sum_{v=1}^{V} \log_2(1 + SINR_v) \ . \tag{19}$$

- Finally, the above steps are repeated a random number of times, e.g. 100 times (i.e. the set of available users U is selected randomly from the total 3,643 receivers, 100 times), to obtain the average of the achievable sum capacity, which is the sum capacity for case 1 and case 2, for U available users.

It has to be noted that the $SINR_{v,DL/UL}$ and $SINR_v$ differ mainly because of the direction of the strongest beam Φ_v in the UL or DL, which depends on the UL or DL channel coefficients (in other words, the strongest cluster in the UL or DL) used for its computation. Also, the users selected by the BS to be served will receive the same power, irrespective of whether the directional information of the UL or the DL is used for DL channel estimation. It should also be noted that in the case when each user has only one dominant cluster in the UL and DL, associated with the same physical IO, the sum capacities of case 1 and case 2 will be the same. The case for the calculation of R_{case1} is equivalent to having the BS knowing the DL channels of all users, which is the case in TDD (i.e., channel reciprocity), and in FDD (when full CSI is fed back). The values obtained, using the above mentioned procedure, are plotted, as shown in Figure 11. The difference between these curves shows the degradation in achievable sum capacity, using UL for DL channel estimation (case 2) and using actual DL channel information (case 1), due to the mismatch between the directional properties of the UL and DL multipath clusters.

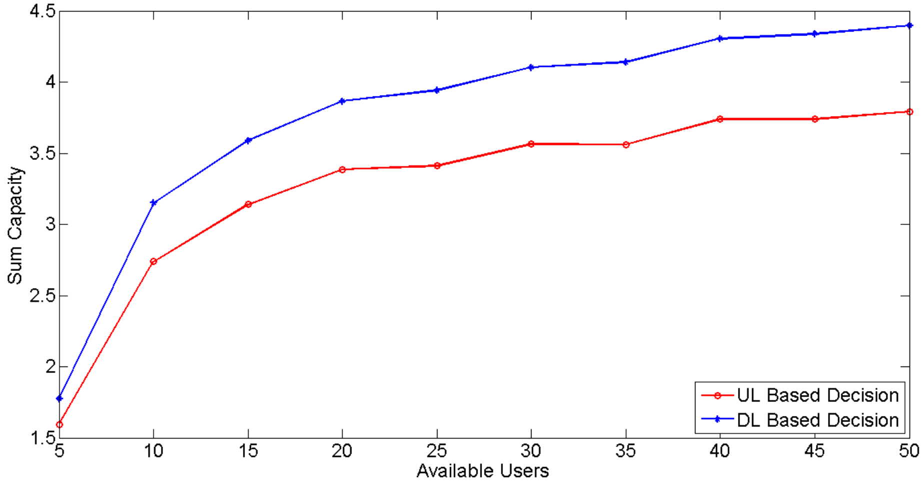

Fig. 11. Achievable sum capacity for different number of users, using N=8 antenna elements in UCA at BS

From Figure 11, it can be seen that the sum capacity calculated from DL based DL estimation, i.e. R_{case1}, is greater than that for UL based DL estimation, i.e. R_{case2}, for all cases. However, the difference is very small when the number of available users is lesser than the number of array elements at the BS, i.e. $U < N$; this is because the BS cannot randomly select the set of users to be served for maximizing the sum capacity, so the sum capacity for case 1 and case 2 will be almost the same. When $U > N$, the BS can select randomly from the set of available users, to serve the best set of users; but in this case, the difference between R_{case1} and R_{case2} is expected to occur because of the mismatch existing between the UL and DL directional channel properties, i.e. $\Phi_{v,UL}$ or $\Phi_{v,DL}$. However, the difference between the sum capacities for UL and DL based decision is quite small; the maximum difference is about 14% with respect to the actual achievable sum capacity. For each case of the number of available users, R_{case2} is very close to R_{case1}. Therefore, the DL beamforming can be performed reliably using the UL channel based DL estimation in FDD systems.

5.3 Relationship between the D_{SDM} and the beamforming algorithm's performance

To study the relationship between the spectral dissimilarity metric introduced in the earlier chapters, and the performance of the beamforming algorithm, we compare the difference of the sum-rate capacity calculated for case 1 and case 2 by implementing the beamforming algorithm on the simulated data set. We assume that the set of available users is equal to the number of antenna elements at BS, i.e. $U = N = 8$. The beamforming algorithm is applied at the BS in the same manner as explained in section 5.2, and then the difference in the sum-rate capacity for UL based DL estimation (case 2) and DL based DL estimation or actual DL channel information (case 1) is evaluated. Once this is done, the introduced metric is used to compare the degradation in the achievable sum capacity based on the difference of the UL and DL multipath cluster properties.

In order to relate the degradation in sum-rate capacity using the introduced beamforming algorithm to the spectral dissimilarity metric, the D_{SDM} is calculated for the multi-user case, considering only the most significant clusters of the UL and the corresponding cluster of DL. The definition of D_{SDM} presented in (6) is for a single-user case, where the number of clusters must always be greater than 1. In the multi-user case, this definition of D_{SDM} is modified in the following way:

$$D_{SDM} = \frac{1}{2}\sum_{n=1}^{N}\left|S_{n,UL} - S_{n,DL}\right| \tag{20}$$

where,

$$S_{n,UL/DL} = \frac{\left|\sum_{l=1}^{L}\alpha_{n,l}^{\;UL/DL}\exp(j\varphi_{n,l}^{\;UL/DL})\right|^2}{\sum_{n'=1}^{N}\left|\sum_{l=1}^{L}\alpha_{n',l}^{\;UL/DL}\exp(j\varphi_{n',l}^{\;UL/DL})\right|^2} \tag{21}$$

Here, instead of calculating the instantaneous cluster power for each cluster of UL or DL that belong to the same user, the instantaneous cluster power is calculated for only the most significant UL/DL cluster for each user in the selected group. As mentioned earlier, the number of available users U is set to be equal to the array elements N, i.e. $U = N = 8$, and the available users are selected randomly, 1000 times, from the set of 3,643 total users. The value of D_{SDM} is calculated for each selected set of users and the sum capacity using UL based DL estimation, as well as the DL based DL estimation is also calculated. Figure 12 shows the scatter plot of the results obtained after 1000 random trials, for values of D_{SDM} and the absolute difference of sum capacities using DL based DL estimation, i.e. R_{case1}, and

UL based DL estimation, i.e. R_{case2}. Table 4 presents the results for the probability of the absolute difference of sum capacity using UL based DL estimation i.e. R_{case2}, and DL based DL estimation, i.e. R_{case1}, to be bound by a certain threshold, for specific ranges of the spectral dissimilarity metric D_{SDM}. The presented results are plotted in Figure 13.

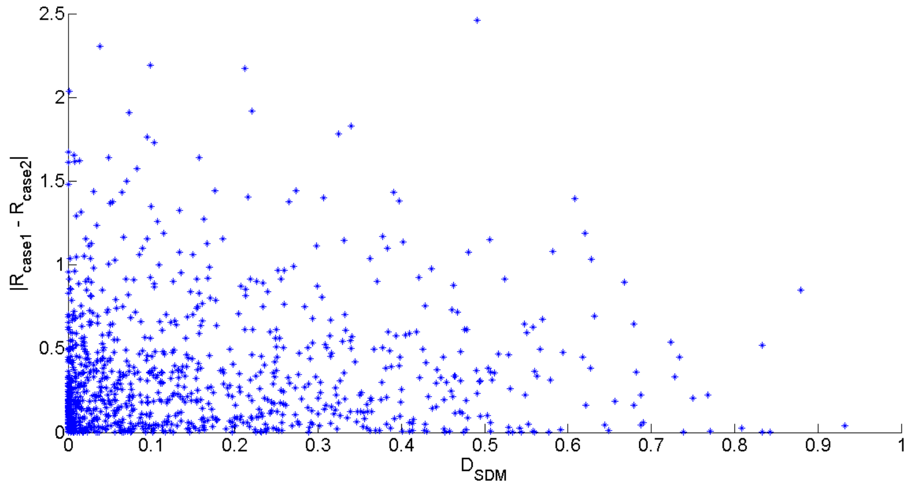

Fig. 12. Scatter plot of the absolute difference between the sum capacities for case 1 and case 2, versus the D_{SDM} values, for 1000 trials, using U = N = 8

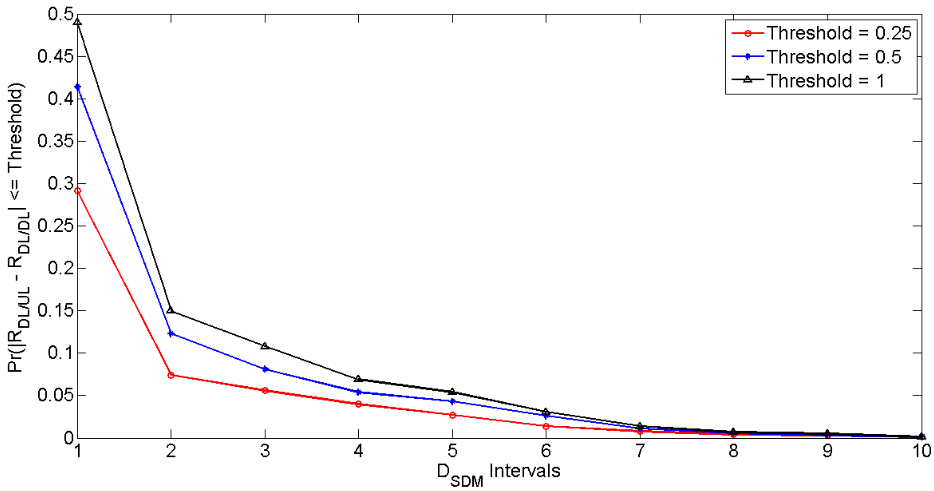

Fig. 13. Plot of the probability of the absolute difference between the sum capacities for case 1 and case 2, to be below a threshold value, versus the D_{SDM} intervals

TABLE 4. COMPARISON OF THE ABSOLUTE DIFFERENCE BETWEEN THE ACHIEVABLE SUM CAPACITIES WITH DIFFERENT RANGES FOR D_{SDM}

Interval No.	**Interval of D_{SDM}**	**Pr ($\|R_{case1}$- $R_{case2}\| \leq 0.25$)**	**Pr ($\|R_{case1}$- $R_{case2}\| \leq 0.5$)**	**Pr ($\|R_{case1}$- $R_{case2}\| \leq 1$)**
1	0 - 0.1	0.291	0.414	0.490
2	0.1 – 0.2	0.074	0.123	0.150
3	0.2 – 0.3	0.056	0.081	0.108
4	0.3 – 0.4	0.040	0.054	0.069
5	0.4 – 0.5	0.027	0.043	0.054
6	0.5 – 0.6	0.014	0.026	0.031
7	0.6 – 0.7	0.008	0.011	0.014
8	0.7 – 0.8	0.004	0.006	0.007
9	0.8 – 0.9	0.003	0.003	0.005
10	0.9 - 1	0.001	0.001	0.001

The scatter plot in Figure 12 shows that the absolute difference between sum capacities for the two cases, i.e., $|R_{case1} - R_{case2}|$, is lesser when the value of D_{SDM} is lesser, since more values are concentrated in the bottom left corner of the plot. In other words, the lesser the spectral dissimilarity metric, lesser is the difference between the sum capacities for UL based DL estimation and DL based DL estimation. This is validated by the results presented in Figure 13 and Table 4.

Figure 13 is the graphical illustration of the results presented in Table 4. The range of D_{SDM} specified in different intervals in Table 4 is shown on the horizontal axis of the plot in Figure 13, whereas the vertical axis shows the probability of the difference between the two capacities, R_{case2} and R_{case1}, to be bounded by a certain value specified as threshold. For example, if the value of D_{SDM} is in the range of 0 – 0.1, i.e. interval 1, the probability that the absolute difference between R_{case1} and R_{case2} to be less than or equal to 1 bps is about 49 %; for interval 2 (i.e., D_{SDM} is in the range 0.1 – 0.2), it is 15% and so on.

From Table 4 and Figures 12 and 13, it can be seen that the mismatch in the UL and DL cluster properties has a great influence on the difference of the achievable sum capacity using UL or DL cluster properties for DL estimation. For almost perfect match between the UL and DL cluster properties, i.e. when D_{SDM} is greater than 0 but lesser than or equal to 0.1, the probability of the absolute value of difference between R_{case1} and R_{case2} below 0.25 bps is much greater as compared to the case when the D_{SDM} is between 0.1 and 0.2. The same can be observed for $|R_{case1} - R_{case2}| \leq 0.5$ and $|R_{case1} - R_{case2}| \leq 1$. Thus, from the results in Table 4 and the sum capacity plot shown in Figure 11, the assumption of improvement in DL channel estimation using UL directional properties in FDD systems, when the mismatch in UL and DL channel properties is small, is validated.

CHAPTER 6

6 Conclusions

This study was based on the possibility of using the directional properties of the multipath clusters in order to improve the DL beamforming transmission in FDD systems without using the feedback. The different MPCs arriving at the BS are seen as clusters on a system level, where each cluster is composed of MPCs possessing similar directional properties. The MPC data is extracted from two methods: using the actual channel measurements, as well as ray-tracing simulations. Two measurement campaigns are conducted to collect the measurement data. The MPC data collected from the first set of actual channel measurements composed of the AAoD, EAoD and complex amplitude for each MPC, whereas from the second data set, the AAoA, EAoA and complex amplitude of each MPC are collected. From the ray-tracing simulations, since the full channel information at both the BS and MS are available, therefore AAoA, EAoA, AAoD, EAoD and complex amplitude of each MPC is collected from the generated output files. Each of the MPC data set is processed using the K-power means clustering algorithm, and the resulting clusters are used for further processing and analysis.

In order to use the UL directional properties for DL channel estimation, it is necessary to characterize the difference between the powers carried by the different multipath clusters between UL and DL. A 'spectral dissimilarity metric', denoted by D_{SDM}, is introduced as a measure to quantify this difference and its usefulness in different propagation scenarios is also discussed. In general, it is observed that the value of D_{SDM} degrades with the increasing number of clusters because as the significance of the power carried by the clusters decreases, the difference between the power of the UL and DL multipath clusters increases. The D_{SDM} for all data sets are computed and plotted as CDFs. For the first set of measurements, the D_{SDM} for 2 most significant UL clusters is found to be less than 0.17, 50% of the time, for all measurements; less than 0.23 for 3 clusters and less than 0.25 for 4 clusters, for all measurements. For the second set of measurements, for 2 most significant clusters, for 50% of the time, the D_{SDM} is less than 0.32; less than 0.44 and 0.5 for 3 and 4 most significant clusters, respectively. The difference in the dissimilarity metric is due to the fact that the propagation environment, the degree of interaction with the IOs, and the effect of the diffused MPCs were different for both the measurement campaigns.

In case of ray-tracing simulations, since mainly the specular propagating waves are considered, the dissimilarity metric has a much lesser value than that for the actual channel measurement. For ray-tracing simulation, the D_{SDM} is less than 0.08 for 50% of the time, for all receiver locations, for all duplex distances, using 2 most significant clusters. For 3 and 4 significant clusters, the D_{SDM} is less than 0.13 and 0.14, respectively. From the above mentioned results, it is found that under favorable propagation scenarios, the directional properties of the DL multipath clusters can be estimated from the UL channel with high reliability. That is why the directional-based beamforming transmission technique for FDD systems will be able to benefit from such similarity in order to improve the system performance.

To further validate the usefulness of the spectral dissimilarity metric, the beamforming algorithm is applied on a simulated data set. The simulated data is collected for a large number of receiver locations, and the beamforming algorithm is applied on the collected parameters for MPCs for all receiver locations. The sum capacity of the overall system is calculated assuming different number of available users, ranging from 5 to 50 users in steps of 5 users, using both the UL based DL estimation and the actual DL channel information. The results illustrate that the sum capacities calculated using UL based DL channel estimation and DL based DL channel estimation are fairly close to each other; the maximum difference is about 14% compared to the sum capacity calculated using actual DL channel parameters. The difference between the capacities arises due to the difference in the directional properties of UL and DL channels, i.e. the selection of the direction of the steering vector based on the strongest beam in UL or DL. It is also worth mentioning that only directional precoding at the BS is used for calculating the sum capacity for the actual DL channel. The achievable sum capacity for UL and DL based DL channel estimation is then calculated for 8 available users, and is related to the spectral dissimilarity metric, D_{SDM}, calculated using the most significant clusters of UL and DL channels, for a large number of sample experiments. The results show that the UL channel can be reliably used for DL channel estimation when the mismatch between the directional properties of multipath clusters is low, which is a typical case. Thus, under favorable propagation conditions, it is possible to estimate the DL channel parameters using the UL channel characteristics in FDD systems, without using the feedback for providing CSIT.

References

[1] Y. Han, J. Ni, and G. Du. "The potential approaches to achieve channel reciprocity in FDD system with frequency correction algorithms." *Communications and Networking in China (CHINACOM), 2010 5th International ICST Conference on*, pp. 1–5, 25-27 August 2010.

[2] L. Bigler, H.-P. Lin, S. S. Jeng, G. Xu, "Experimental direction of arrival and spatial signature measurements at 900 MHz for smart antenna systems," *Vehicular Technology Conference, 1995 IEEE 45th*, vol.1, pp. 55–58, 25-28 July 1995.

[3] K. I. Pedersen, P. E. Mogensen, and F. Frederiksen, "Joint directional properties of uplink and downlink channel in mobile communications," *Electronics Letters*, vol.35, no.16, pp. 1311–1312, 5 August 1999.

[4] S. E. Foo, M. A. Beach, P. Karlsson, P. Eneroth, B. Lindmark, J. Johansson, "Spatio-temporal investigation of UTRA FDD channels," *3G Mobile Communication Technologies, 2002. Third International Conference on (Conf. Publ. No. 489)*, pp. 175–179, 8-10 May 2002.

[5] M. Haardt, 1996, "Efficient one-, two-, and multidimensional high-resolution array signal processing", PhD. Thesis, Ilmenau, Germany, ISBN 3-8265-2220-6.

[6] K. Hugl, K. Kalliola and J. Laurila, "Spatial Reciprocity of UL and DL Radio Channels in FDD Systems," COST 273 TD(02)066Espoo, Finland, 2002/May/30-31.

[7] A. F. Molisch, *Wireless Communications*, Wiley, 2011.

[8] J. Vieira, "*Tracking of multipath delays for UWB based positioning*," Master's Thesis, Department of Electrical and Information Technology, LTH, Lund University, July 2013.

[9] S. Wyne, N. Czink, J. Karedal, P. Almers, F. Tufvesson, and A. F. Molisch, "A cluster-based analysis of outdoor-to-indoor office MIMO measurements at 5.2 GHz," *Vehicular Technology Conference, 2006. VTC-2006 Fall 2006 IEEE 64th*, pp. 1–5, 25-28 September 2006.

[10] A. Saleh and R. A. Valenzuela, "A statistical model for indoor multipath propagation," *IEEE J. Selected Areas Comm.*, vol. 5, pp. 128–137, February 1987.

[11] J. Fuhl, A. F. Molisch, and E. Bonek, "Unified channel model for mobile radio systems with smart antennas," in *Proc. IEE Radar, Sonar and Navigation*, vol. 145, pp. 32–41, IEE, February 1998.

[12] A. Molisch, "Modeling the MIMO propagation channel," *Belgian Journal of Electronics and Communications*, no.4, pp. 5–14, 2003.

[13] C.-C. Chong, C.-M. Tan, D. Laurenson, S. McLaughlin, M. Beach, and A. Nix, "A new statistical wideband spatio-temporal channel model for 5-GHz band WLAN systems," *IEEE Journal on Selected Areas in Communications*, vol.21, no.2, pp. 139–150, February 2003.

[14] N. Czink, P. Cera, J. Salo, E. Bonek, J.-P. Nuutinen, J. Ylitalo, "A Framework for Automatic Clustering of Parametric MIMO Channel Data Including Path Powers," *Vehicular Technology Conference, 2006. VTC-2006 Fall. 2006 IEEE 64th*, pp. 1-5, 25-28 September 2006.

[15] N. Czink, P. Cera, J. Salo, E. Bonek, J.-P. Nuutinen, and J. Ylitalo,"Automatic clustering of MIMO channel parameters using the multipathcomponent distance measure," in Proc. *WPMC2005*, Aalborg, Denmark, September 2005, pp. 829-833.

[16] R. Bultitude, G. Brussaard, M. Herben, and T. Willink, "Radio channel modellingfor terrestrial vehicular mobile applications," *Millennium Conference in Antennas and Propagation*, Davos, Switzerland, April 2000.

[17] I. E. Teletar, "Capacity of multi-antenna gaussian channels," *Eur. Trans. Telecommun.*, vol.10, no.6, pp. 585-595, 1999.

[18] G.S. Dahman, R. H. M. Hafez, "Angle-of-Departure-Aided Opportunistic Space-Division Multiple Access," *Communication Networks and Services Research Conference, 2009. CNSR '09. Seventh Annual* , pp. 146-152, 11-13 May 2009.

[19] R. S. Thomä, D. Hampicke, A. Richter, G. Sommerkorn, A. Schneider, U. Trautwein, and W. Wirnitzer, "Identification of time-variant directional mobile radio channels," *Instrumentation and Measurement, IEEE Transactions on*, vol.49, no.2, pp. 357-364, April 2000.

[20] G. Xiang, F. Tufvesson, O. Edfors, F. Rusek, "Measured propagation characteristics for very-large MIMO at 2.6 GHz," *Signals, Systems*

and Computers (ASILOMAR), 2012 Conference Record of the Forty Sixth Asilomar Conference on , pp. 295–299, 4-7 November 2012.

[21] J. Flordelis, G. Dahman, F. Tufvesson, ”Measurements of Large-Scale Parameters of a Distributed MIMO Antenna System in a Microcell Environment at 2.6 GHz,” *Antennas and Propagation (EuCAP), 2013 7th European Conference on*, pp. 3026–3030, 8-12 April 2013.

[22] 3GPP TS 36.101 version 11.6.0 Release 11, accessed from: http://www.3gpp.org/DynaReport/36101.htm, accessed on February 2, 2014.

[23] Wireless InSite Reference Manual, Remcom Inc., Version 2.6.3, November 2012.

[24] P. Ioannides, and C. A. Balanis, “Uniform circular arrays for smart antennas,” *IEEE Antennas and Prop. Mag.*, vol.47, no.4, pp. 192 – 206, August 2005.

[25] B. Fleury, Y. Xuefeng, K. Rohbrandt, P. Jourdan, and A. Stucki, “Performance of a high-resolution scheme for joint estimation of delay and bidirection dispersion in the radio channel,” *IEEE 55th VTC 2002* Spring, May 6- 9, Birmingham, Alabama, USA, pp. 522 – 526.

[26] N. Blaunstein, M. Toeltsch, J. Laurila, E. Bonek, D. Katz, P. Vainikainen, N. Tsouri, K. Kalliola, and H. Laitinen, “Signal power distribution in the azimuth, elevation and time delay domains in urban environments for various elevations of base station antenna,” *IEEE Trans. Antennas Propag.*, vol.54, pp. 2902 – 2916, October 2006.

List of Figures

List of Tables

List of Acronyms

BS	Base Station
E-UTRA	Evolved Universal Terrestrial Radio Access
FDD	Frequency Division Duplex
LOS	Line-of-Sight
MIMO	Multiple-Input Multiple-Output
MPC	Multi-Path Component
MS	Mobile Station
NLOS	Non Line-of-Sight
TDD	Time Division Duplex
UCA	Uniform Circular Array
UMTS	Universal Mobile Telecommunications System
WCDMA	Wideband Code Division Multiple Access

LUND UNIVERSITY

http://www.eit.lth.se